Structures 50 (2023) 148–160

Contents lists available at ScienceDirect

Structures

journal homepage: www.elsevier.com/locate/structures

Dynamic identification of brick masonry semi-circular arches due to temperature and moisture

Alireza Alaei [a], Mehrdad Hejazi [a,*], Elizabeth Vintzilaiou [b], Androniki Miltiadou-Fezans [c], Marek Skłodowski [d]

[a] Department of Civil Engineering, Faculty of Civil Engineering and Transportation, University of Isfahan, Isfahan, Iran
[b] School of Civil Engineering, National Technical University of Athens, Athens, Greece
[c] School of Architecture, National Technical University of Athens, Athens, Greece
[d] Institute of Fundamental Technological Research, Polish Academy of Sciences, Warsaw, Poland

ARTICLE INFO

Keywords:
Operational Modal Analysis
Brick Masonry Semi-Circular Arch
Temperature
Moisture
Dynamic Parameters

ABSTRACT

This paper presents the effects of changes in temperature and moisture content on the dynamic properties of semi-circular arches made of clay brick and gypsum mortar constructed and tested in the laboratory. First, the mechanical properties of the materials used were determined by experimental tests. Operational Modal Analysis was then performed for each condition to measure natural frequencies, mode shapes, and modal damping ratios. An empirical equation for estimating the natural frequencies of the studied arch at different material moisture contents was proposed using the obtained results from experimental tests. Finally, the Finite Element Model Updating Method (FEMU) was applied to calibrate some of the material mechanical properties in modelled arches. In contrast to the effect of moisture, temperature changes showed a difficulty to interpret effect on the dynamic properties of the arch. On the other hand, Poisson's ratio did not affect the dynamic behaviour of the specimen.

1. Introduction

Preservation of the architectural heritage is necessary because of its cultural importance to humans. Arches are very frequently met in architectural heritage structures to be preserved. In Persian architecture, arches made of bricks and gypsum mortar constitute typical structural elements. Various geometries are used, the most common being that of semi-circular arches (Fig. 1).

The dynamic identification method is a non-destructive method used for identifying the dynamic properties of structures. In studying heritage structures, dynamic identification as a non-destructive method is helpful in evaluating the current structural condition and selection of restoration techniques. Dynamic parameters may be affected by factors such as temperature, moisture content. Identifying and differentiating the effect of each of the factors mentioned can help to better understand the structural condition.

Techniques for the dynamic identification of structures have been used in research and practice since 1980 [1]. Several applications in the last two decades have repeatedly demonstrated the possibilities offered by those techniques. Thus, Jaishi et al. [2] determined the dynamic properties of a three-story temple in Nepal using dynamic vibrations. In addition to the advantages of the ambient vibration method, they stated that this method was proven to be sufficient to calculate the main modes of the structure. De Sortis et al. [3] checked the ability of dynamic identification procedure, usually applied to engineering buildings, to estimate the dynamic behaviour of existing masonry buildings. They concluded that dynamic identification techniques could provide valuable information about the dynamic properties of existing masonry structures. On the other hand, Ramos et al. [4] were the first to establish a relationship between the damage process and the dynamic response of a masonry structure. Gentile and Saisi [5] obtained the five primary modes of a masonry bell-tower by measuring the vibration caused by wind, using twenty uniaxial sensors. Other researches on towers include the works of Rebelo et al. [6] who used modal identification based on Operational Modal Analysis (OMA) to calibrate the FE model of an old stone masonry tower, and of Ivorra and Pallarés [7] who determined the bending and torsional natural frequencies and damping ratio of a historical masonry bell tower. Obtained data were used in a numerical

* Corresponding author.
E-mail addresses: a.alaei@trn.ui.ac.ir (A. Alaei), m.hejazi@eng.ui.ac.ir (M. Hejazi), elvintz@central.ntua.gr (E. Vintzilaiou), amiltiadou@arch.ntua.gr (A. Miltiadou-Fezans), msklod@ippt.pan.pl (M. Skłodowski).

https://doi.org/10.1016/j.istruc.2023.02.022
Received 13 August 2022; Received in revised form 19 January 2023; Accepted 5 February 2023
Available online 13 February 2023

Fig. 1. A semi-circular arch made of clay brick and gypsum mortar, Choga Zambil, Susa, 1250 BCE.

model of the tower to assess its dynamics performance before and after restoration. Makarios [8,9] presented a method that was able to identify the dynamic properties of tall buildings due to seismic excitation and wind loading. Foti et al. [10] were able to obtain five main modes of a historical tower by performing OMA and signal processing using the Frequency Domain Decomposition (FDD) method. Gentile and Saisi [11] performed two OMA tests on a bell tower using two different types of excitation forces.Masciotta et al. [12] studied the dynamic properties, including natural frequencies and mode shapes, of a historical brick masonry chimney using the Stochastic Subspace Identification (SSI) method and studied the effect of occurred damages on it.

Valvona et al. [13] investigated the effect of strengthening a historical vault using cement with glass fibres using dynamic identification. Mesquita et al. [14] investigated the reliability of retrofitting a masonry heritage construction using OMA. Cavalagli et al. [15] investigated the advantages of vibrational health monitoring in detecting small failures caused by mild earthquakes with a short return period. Vincenzi et al. [16] investigated the health monitoring of a bell tower. Their goal was to obtain the tension generated in the tower due to the vibration of the bell. The calibrated finite element (FE) model of the structure was obtained by performing vibrational monitoring tests on the structure and model updating. Bianchini et al. [17] studied the seismic performance of a temple. They used dynamic identification to calibrate the numerical model and evaluated a strengthening technique with stainless steel ties to improve the seismic behaviour. Onat [18] developed an empirical equation to fit the natural frequency of historical masonry bridges. He used the experimental data obtained from ambient vibration identification. Nochebuena-Mora et al. [19] studied the dynamic effects of bell swinging on a masonry tower using dynamic identification tests and calibrated the numerical model of the tower. Calayır et al. [20] updated the finite element model of masonry minarets by using dynamic properties obtained from OMA tests. They also considered structure-foundation-soil interaction during the updating. Gonen and Soyoz [21] determined the modulus of elasticity of a stone masonry wall using empirical equations, mechanical tests, ambient vibration tests and model updating, and highlighted the uncertainties. Lately the probabilistic approaches in model updating made it possible to evaluate the uncertainties in the identified results [22–24]. Increasing the ability of measurement equipment has made dynamic identification an effective in situ tool for traditional masonry structures. It has also been shown that this non-destructive tool has a practical application in monitoring the changes made in these structures.

This study investigates the effect of the mentioned conditions on the dynamic properties of semi-circular brick arches. Experimental and numerical work was undertaken, structured in several stages, described herein: a) A semi-circular brick masonry arch was constructed in the laboratory using clay bricks and gypsum mortar. The mechanical properties of the materials, namely, compressive strength and modulus of elasticity, were experimentally determined. b) Dynamic properties, such as natural frequencies, mode shapes and modal damping ratios, of the intact arch in standard laboratory conditions (i.e., 20 °C temperature and 11 % moisture content), were measured using the OMA test method. Subsequently, c) the arch temperature was set either to 14 °C or 38 °C. d) The moisture content of the intact arch was set to four values (5 % or 11 % or 18 % or 24 %). After changing each of these conditions, dynamic tests were repeated to measure the dynamic properties. Finally, e) FE models were constructed for the arch. Using the Finite Element Model Updating Method (FEMU), calibrated material properties were obtained and reported for future use in the FE models. These values were also compared with the initial values determined from mechanical tests to highlight the differences between the material properties in dynamic and static conditions.

2. Techniques adopted for dynamic identification and evaluation of results

The dynamic properties of the structure (such as natural frequencies, mode shapes and modal damping ratios) was obtained, using OMA method. Random excitations were used to excite the structure [25]. The Enhanced Frequency Domain Decomposition (EFDD) method was used to calculate the dynamic parameters from the experimentally recorded data [26]. The obtained measurements can be directly evaluated by comparing the values of each dynamic parameter before and after the change of one condition (i.e., changes in temperature and moisture content).

Surveying the change in material properties that govern the dynamic behaviour of the structure using the updated FE model, contributes to the interpretation of the results. FEMU is an optimisation process applied to minimise the difference between the dynamic structure test results and the response of its FE model. Various approaches about applications of this method and its relations are presented in [27]. One of the main issues is selecting the objective function, which is used to check the minimisation process of the difference between experimental and FE results. One suitable objective function for simple structures that uses the values of natural frequencies and mode shapes of experiments and FE models is presented in [28] as Equation (1).

$$\pi = \frac{1}{2}\left[\sum_{j=1}^{N} r_{\omega,j} + \sum_{j=1}^{N}\sum_{i=1}^{m} r_{\varphi,j,i}\right] \tag{1}$$

where π is the objective function, N is the number of modes, m is the number of DOFs in each mode shapes vector and r_ω r_φ are the residuals of frequencies and mode shapes vector, respectively, calculated by Equation (2).

$$r_{\omega,j} = W_{\omega,j}\left(\frac{\omega_j^2 - \omega_{j,\exp}^2}{\omega_{j,\exp}^2}\right)^2; \quad r_{\varphi,j,i} = W_{\varphi,j}\left(\varphi_j^i - \varphi_{j,\exp}^i\right)^2 \tag{2}$$

where W_φ and W_ω are the weighting factors for mode shapes and fre-

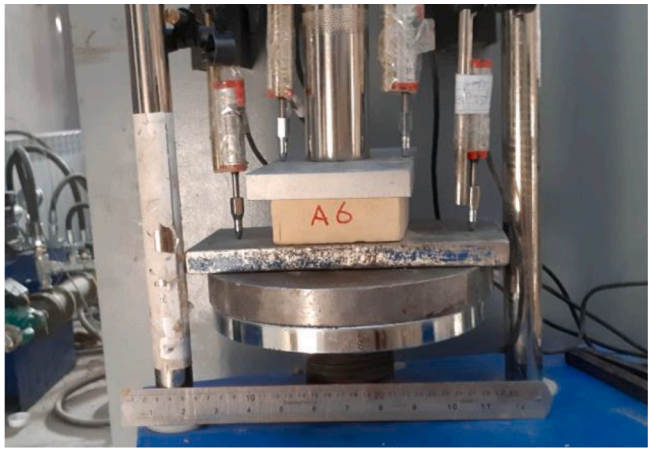

(a)

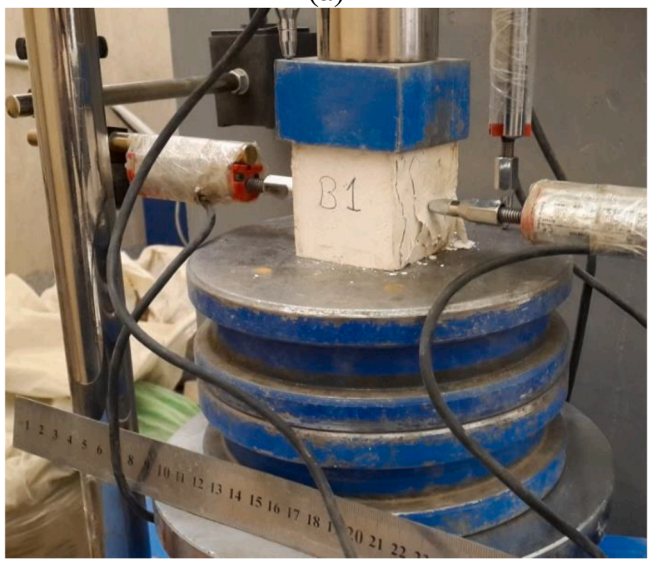

(b)

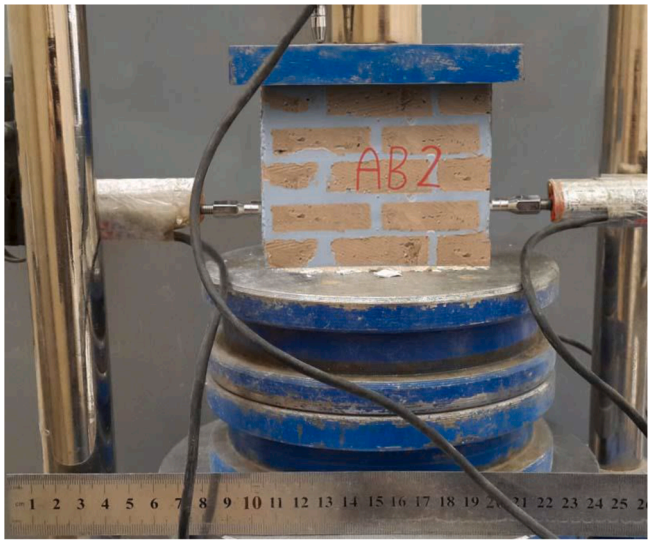

(c)

Fig. 2. Specimens under compression: a) brick, b) gypsum mortar, c) masonry prism.

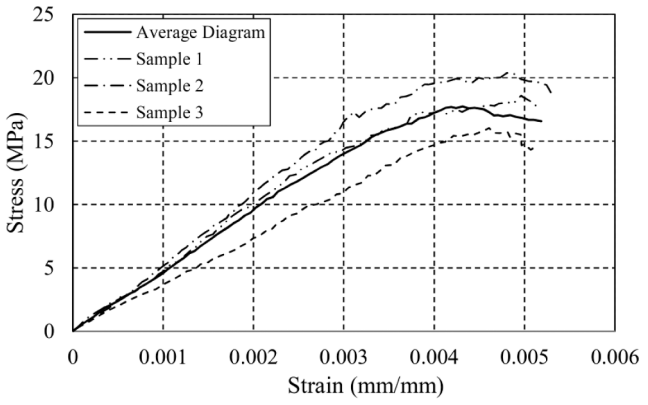

(a)

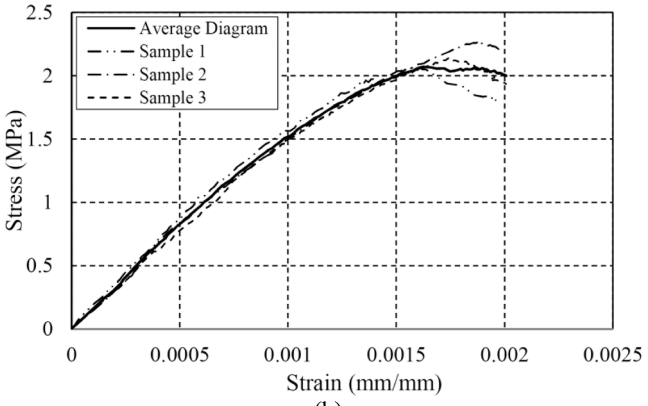

(b)

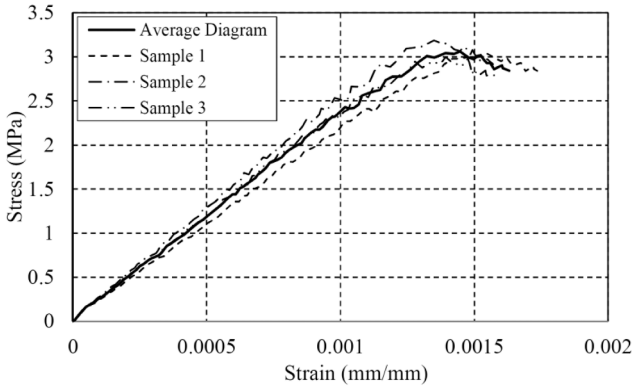

(c)

Fig. 3. Stress–strain diagram of: a) brick, b) gypsum mortar, and c) masonry prism.

Table 1
Properties of used materials.

Material properties	Brick	Gypsum	Masonry prism
Mass density (kg/m^3 kg/m^3)	1565	1200	1466
Modulus of elasticity (MPa)	4603	1659	2586
Compressive strength (MPa)	12.63	1.78	2.21

quencies, respectively, which are selected based on engineering judgment, ω_j and $\omega_{j,\exp}$ are the j^{th} numerical and experimental frequencies, respectively.

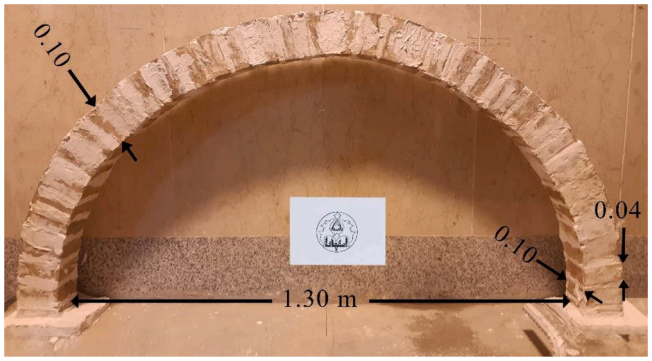

(a)

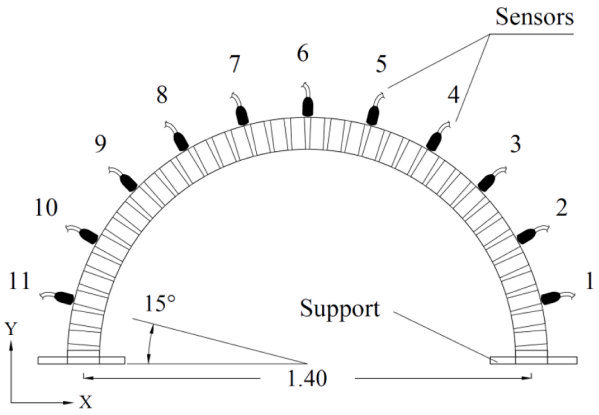

(b)

Fig. 4. Semi-circular arch: a) after construction was completed, b) locations of the sensors.

3. Experimental work

3.1. Materials

Materials mass density measurement and compression tests were performed on material specimens to determine the mechanical properties of materials used to construct the arch. Since the properties of the materials can be different in dynamic conditions than in static ones, the measured properties of materials were used as initial values in the FE model of the semi-circular brick arch under study.

Compression tests were performed on specimens of clay brick and gypsum mortar (after 28 days), as well as on masonry prisms. Three specimens per material were tested in order to measure the modulus of elasticity and the compressive strength. The axial deformation of the

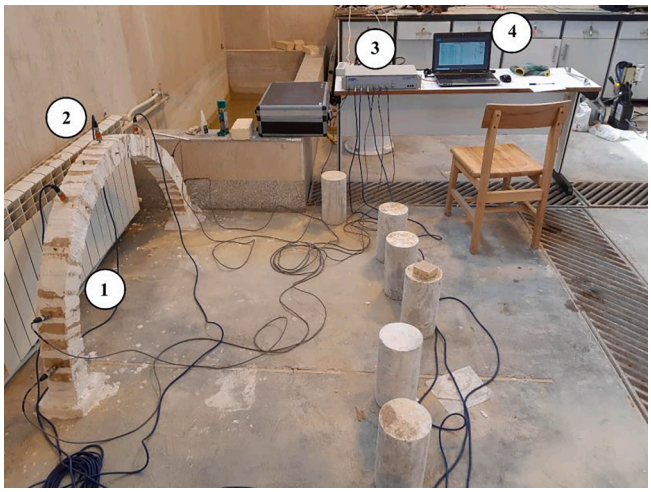

Fig. 6. Dynamic tests: (1) the tested arch, (2) sensors in-place, (3) data logger, (4) laptop.

(a)

(b)

Fig. 5. Arch OMA tests with two sensor arrangements: a) arrangement 1, b) arrangement 2.

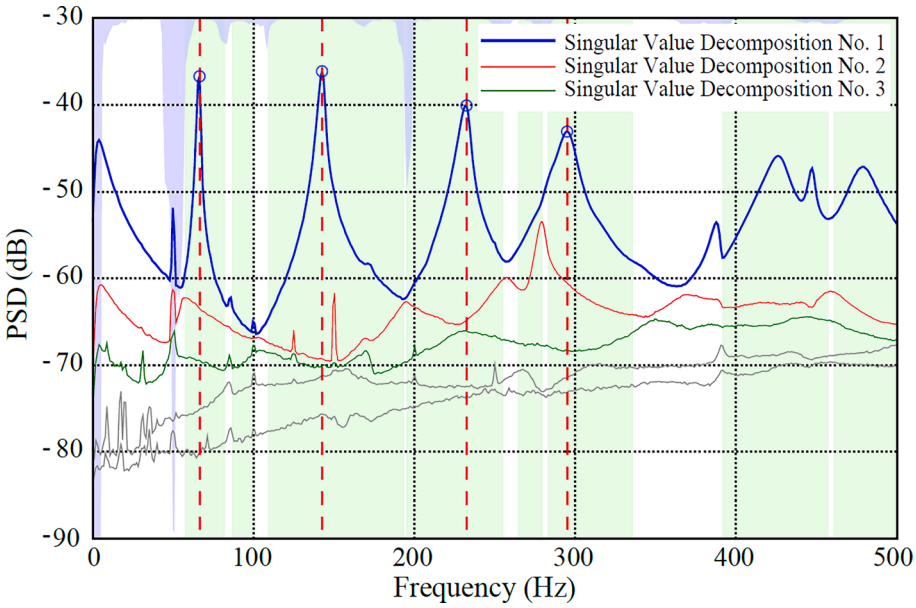

Fig. 7. Power Spectral Density (PSD) of OMA test and obtained frequencies.

Table 2
Frequencies computed for six tests of the semi-circular arch under normal conditions of laboratory (temperature of 20 °C and moisture content of 11 %).

Mode	Test 1	Test 2	Test 3	Test 4	Test 5	Test 6	Average	Standard deviation (σ_ω)
	Frequency (Hz)							
1	66.2	65.4	65.7	65.4	65.4	64.5	65.4	0.56
2	143.3	142.1	144.3	142.1	142.1	139.6	142.3	1.56
3	232.4	232.7	233.4	230.5	229.5	224.1	230.4	3.44
4	295.9	296.0	295.2	293.0	290.5	279.8	291.7	6.21

Table 3
Modal damping ratios computed for six tests of the semi-circular arch under normal conditions of laboratory (temperature of 20 °C and moisture content of 11 %).

Mode	Test 1	Test 2	Test 3	Test 4	Test 5	Test 6	Average	Standard deviation (σ_ω)
	Frequency (Hz)							
1	1.2	0.8	0.8	1.1	0.8	0.9	0.9	0.16
2	1.2	1.7	1.7	0.9	1.1	1.1	1.3	0.34
3	1.4	1.5	1.5	1.4	1.5	2.0	1.5	0.22
4	2.1	2.0	2.0	1.1	3.0	1.7	2.0	0.59

tested specimens was recorded using LVDTs, as shown in Fig. 2. The tests were performed according to BS EN 772–1 [29], BS EN 13279–2 [30] and BS EN 1052–1[31] for bricks, mortar and masonry prism respectively.

Fig. 3 shows the compressive stress versus vertical strain curves obtained from testing the conventional specimens. The modulus of elasticity is the secant modulus at 30 % of the maximum resistance [31]. The obtained stress–strain relationships for brick, gypsum mortar, and masonry prism are as Equations (3), (4) and (5), respectively, where σ is the stress and ε is the strain, and subscripts b, g and m indicate brick, gypsum mortar and masonry prism, respectively.

$$\sigma_b = -2\times10^{10}\times\varepsilon_b^4+4\times10^7\times\varepsilon_b^3+2.015\times10^5\times\varepsilon_b^2+4.33\times10^3\times\varepsilon_b+0.15 \quad (3)$$

$$\sigma_g = -6.57\times10^{10}\times\varepsilon_g^4+5.31\times10^7\times\varepsilon_g^3+2.34\times10^5\times\varepsilon_g^2+1.79\times10^3\times\varepsilon_b+0.01 \quad (4)$$

$$\sigma_m = -9.55\times10^{11}\times\varepsilon_m^4+2.09\times10^9\times\varepsilon_m^3-1.47\times10^6\times\varepsilon_m^2+2.71\times10^3\times\varepsilon_m+0.002 \quad (5)$$

The modulus of elasticity is taken as the average of the three experimental values, according to BS EN 1052-1 [31].

The compressive strength of the masonry prism is calculated from the average compressive strength of the specimens (Table 1). The measured mass density, modulus of elasticity and compressive strength for tested materials are also presented in Table 1.

It is well known that the modulus of elasticity of masonry materials under vibration is different from those related to static tests [32]. Therefore, the obtained values from testing were used as initial values in the FE model of the semi-circular brick masonry arch. Those initial values were updated, in the course of the calculations, until the numerical results matched the experimental ones.

3.2. Construction of the arch and instrumentation

A semi-circular arch was constructed in the laboratory using bricks

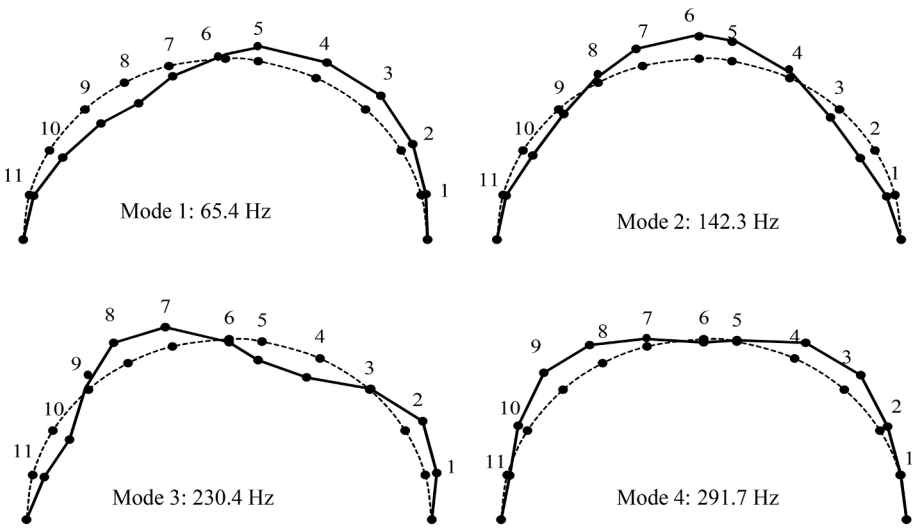

Fig. 8. The arch deformation for each mode, obtained from OMA under normal in-lab conditions (temperature of 20 °C and moisture content of 11 %).

(a)

(b)

Fig. 9. Changing the temperature and performing OMA test on the arch: a) covered arch, b) OMA testing of the arch.

and gypsum mortar, i.e., materials that were frequently used in arch construction in Persian historical monuments (e.g., Jami mosque of Isfahan). Traditional hand-made fired clay bricks were used, 100 mm long, 100 mm wide, and 40 mm thick, and gypsum mortar was used in trapezoidal joints (with an average thickness of 15 mm). The internal radius of the arch is equal to 0.65 m, its span 1.40 m, and its height and thickness are equal to 0.10 m. The arch is bonded to the gypsum mortar supports of 100 mm long, 100 mm wide and 20 mm thick, fixed to the ground floor (Fig. 4(a)). The rigidity of supports is numerically checked, through FEMU.

Twenty-eight days after its construction, the arch was provided with sensors, adequate for the dynamic tests. Thus, several accelerometers were installed on the arch. Cyanoacrylate glue was used to fix them at the mid-thickness of the arch. The sensors are piezoelectric with a frequency measurement range of 0.15 Hz to 10,000 Hz. Moreover, their dynamic range and sensitivity are ± 3 g and 1000 mV/g, respectively. These sensors are uniaxial with a weight of 0.110 kg and are connected, using a coaxial cable, to a data acquisition system with a 16 bit ADC. The data acquisition system recorded the data with the sample rate of 2000 Hz.

Numerical calculations were performed with the aim to define the proper number and location of the sensors. To this purpose, ten mode shapes were considered, indicating the eleven points shown in Fig. 4(b), as adequate for the installation of accelerometers. Installation points corresponded to the locations of the maximum magnitudes of the mode shapes. Considering that seven sensors are available, the decision was to duplicate all dynamic tests by adopting two sensor arrangements. Fig. 5 shows the sensors in the first and second arrangements.

The type of excitation force is an important factor in dynamic analysis. In this work, a steel hammer weighing 1.2 kg (4 % of the sample arch mass [33]) was used to excite the structure randomly (in terms of time and location). According to the assumptions related to the OMA test theory, the ideal type of excitation is the white noise or unit impulse. Although random impact seems to violate this assumption, the successful use of this type of excitation and the validity of the obtained results have been reported by other researchers [34].

3.3. Dynamic test of the arch under normal conditions

The first set of (reference) tests were performed on the arch in normal temperature (20 °C) and moisture content (11 %) conditions in the laboratory (at an age of 28 days). Several tests were performed to reduce testing errors and detect vibration modes with enhanced reliability. The final result is the average of the obtained measurements. According to relevant literature, the minimum number of dynamic tests is five [33]. In contrast, the suitable duration for data collection in each test is equal to 2000 times the first period of the structure [35]. Fig. 6 shows the semi-circular arch during the dynamic test.

The natural frequencies were obtained from the frequency spectrum using the EFDD method (Fig. 7). Table 2 and 3 presents the frequencies

Table 4
The natural frequencies of the arch at different temperatures.

Mode	$f_{14^\circ C}$ (Hz)	$f_{20^\circ C}$ (Hz)	$f_{38^\circ C}$ (Hz)	$\Delta f_{14^\circ C,20^\circ C}$ (\%)	$\Delta f_{38^\circ C,20^\circ C}$ (%)	$\Delta f_{38^\circ C,14^\circ C}$ (%)
1	64.1	64.5	66.0	−0.5	2.4	2.9
2	139.3	139.6	134.6	−0.3	−3.6	−3.3
3	225.2	224.1	217.1	0.5	−3.1	−3.6
4	286.4	279.8	294.1	2.4	5.1	2.7

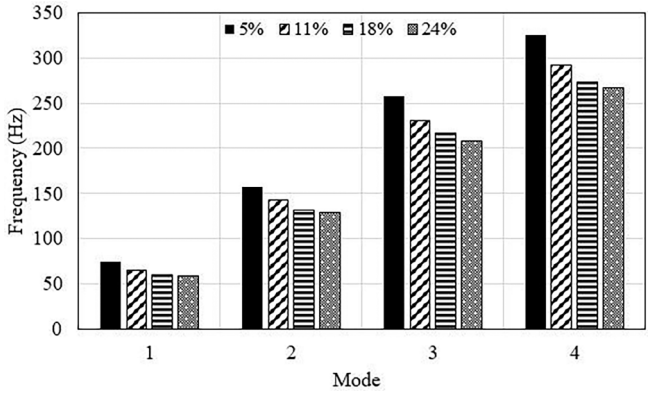

Fig. 10. Comparison of the arch natural frequencies at different moisture contents.

and the modal damping ratios computed for six tests of the semi-circular arch. The average and the standard deviation of the results for the first four vibration modes of the arch are included. Based on the standard deviation of the obtained frequencies, the most stable mode among the four computed modes is the first mode with a frequency of 65.4 Hz. The frequency range for these four modes is from 65.4 Hz to 295.9 Hz (Fig. 7). The modal damping ratios vary from 0.9 % to 2.0 %. The first mode has the minimum modal damping ratio of 0.9 %, and the fourth mode has the maximum modal damping ratio of 2.0 %. The standard deviation indicates that the modal damping ratio varies widely in different tests, unlike frequency values. The semi-circular arch deformation for each mode obtained from the test is illustrated in Fig. 8.

3.4. Effect of temperature on the arch

To study the effect of temperature changes on the dynamic properties of the semi-circular arch, dynamic tests were performed for three values of temperature, namely, 14 °C, 20 °C and 38 °C. Those temperatures were selected accounting for the outside temperature at the testing time and the available heating equipment. To force the temperature to drop to 14 °C indoors, the heating system was kept off for 24 h. On the contrary, to keep the air temperature constant at 20 °C, the radiator was active for a full day. Finally, to raise the air temperature to 38 °C, the arch and space around it were covered to prevent thermal loss (Fig. 9 (a)), while the radiator and an electric heater were continuously on. The temperature has been set at the predefined value, and the operational modal tests were performed. Fig. 9(b) shows the arch after performing the tests and removing the cover.

Table 4 shows the frequencies obtained for each temperature. Table 4 shows that by increasing the temperature from 14 °C to 38 °C, a slight increase of the frequency at the first, and fourth modes (i.e., 2.9 % and 2.7 %, respectively) was recorded. On the contrary, the frequencies of other modes decreased, ranging from −3.6 % for the third mode to −3.3 % for the second mode. Therefore, the change of frequency ranges from −3.5 % to 2.9 % for temperatures between 14 °C and 38 °C. No significant trend was observed for frequency changes due to changes in air temperature within the investigated temperature range. A similar result was reported in [33].

3.5. Effect of moisture content on the arch

To study the effects of material moisture content on the dynamic properties of the semi-circular arch, dynamic tests were first performed for moisture contents of 5 %, 18 % and 24 %, and the natural frequencies and mode shapes of the arch were determined by performing OMA tests for each moisture content. Then, four equations were fitted to the obtained experimental frequencies. These equations can accurately estimate the natural frequencies of the semi-circular arch at different material moisture content.

3.5.1. Experimental study for the effect moisture content on the arch

The arch was subjected to moisture contents of 5 %, 18 %, and 24 % (at 20 °C). They were compared with the results obtained from normal moisture content conditions, i.e., 11 %. In order to reduce the moisture content to 5 % (6 % lower than normal condition), the arch was kept in a thermal chamber (Fig. 9(a)) for 24 h. Then, water was sprayed onto the arch in several steps to create 18 % and 24 % moisture content (7 % and 13 % higher than normal condition, respectively). The steps were conducted 5 h later to ensure a better moisture uniformity in the entire arch. A masonry prism was used as a control sample (subjected to the same conditions as the arch) to measure the moisture content. After the moisture content was set to the predefined values, OMA tests were performed, and the natural frequencies and mode shapes for the first four modes of the arch were calculated. Fig. 10 shows that there is a trend for the frequencies to decrease with increasing moisture content, whereas this decrease seems to be more pronounced for moisture content increasing from 5 % to 11 %. The frequency values calculated for the examined cases and the difference to the normal moisture content of 11 % are presented in Table 5. It is observed that the natural frequencies of all modes have continuously decreased by increasing the moisture content from 5 % to 24 %.

Moreover, the frequency drop is more considerable for low moisture contents than for high moisture contents. The frequencies have decreased by about 14 % for moisture content increase from 5 % to 11 %. They have decreased by only about 3 % for moisture increase from

Table 5
The natural frequencies of the arch at different moisture contents.

Mode	Moisture content				$\Delta f_{5\%,11\%}$ (%)	$\Delta f_{18\%,11\%}$ (%)	$\Delta f_{24\%,11\%}$ (%)
	5 %	11 %	18 %	24 %			
1	74.4	65.4	59.7	58.4	13.7	−8.8	−10.7
2	157.7	142.3	131.0	128.9	10.9	−7.9	−9.4
3	257.9	230.4	216.1	207.8	11.9	−6.2	−9.8
4	325.7	291.7	273.1	266.5	11.7	−6.4	−8.7

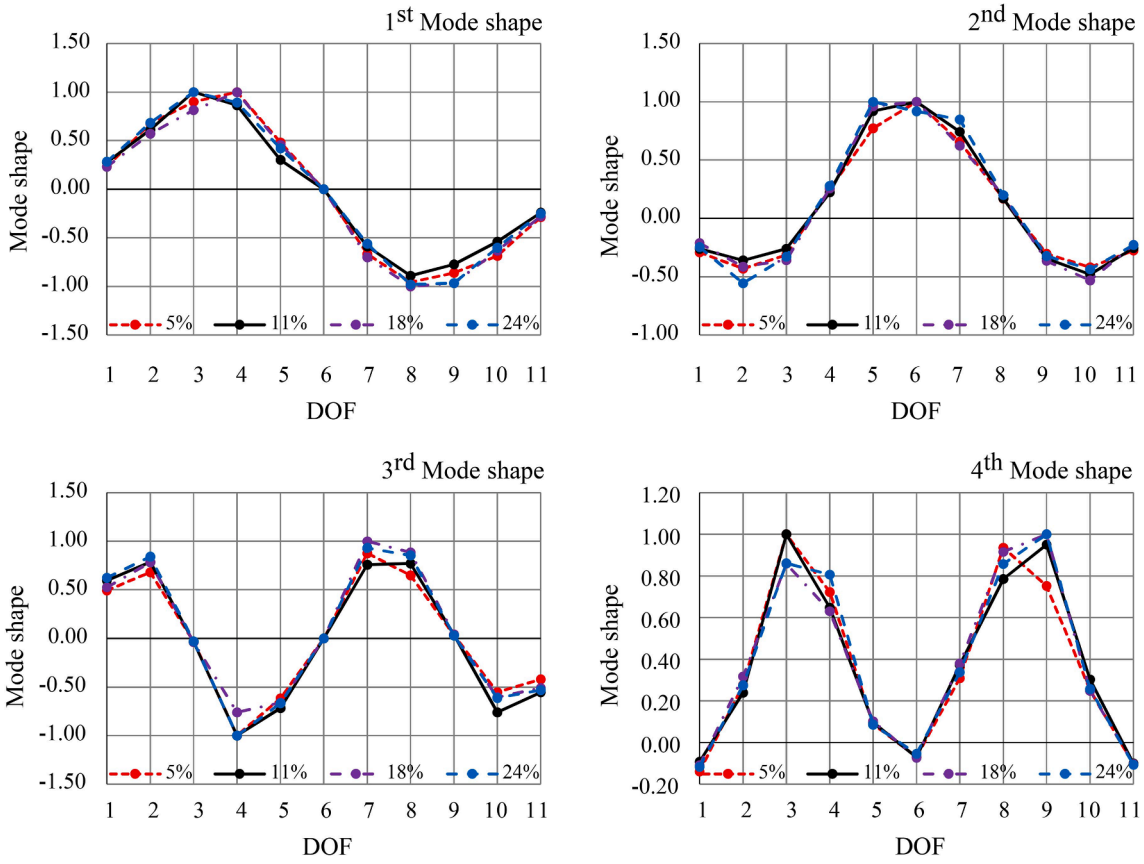

Fig. 11. Comparison of the normalised mode shapes of the arch at different moisture contents.

Table 6
The used set of data for fitting the equation for estimating the natural frequencies of the arch at different material moisture contents.

Number	m_0(%)	m(%)	Mode 1		Mode 2		Mode 3		Mode 4	
			f_0(Hz)	f(Hz)	f_0(Hz)	f(Hz)	f_0(Hz)	f(Hz)	f_0(Hz)	f(Hz)
1	5	5	74.4	74.4	157.7	157.7	257.9	257.9	325.7	325.7
2	5	11	74.4	65.4	157.7	142.3	257.9	230.4	325.7	291.7
3	5	18	74.4	59.7	157.7	131	257.9	216.1	325.7	273.1
4	5	24	74.4	58.4	157.7	128.9	257.9	207.8	325.7	266.5
5	11	5	65.4	74.4	142.3	157.7	230.4	257.9	291.7	325.7
6	11	18	65.4	59.7	142.3	131	230.4	216.1	291.7	273.1
7	11	24	65.4	58.4	142.3	128.9	230.4	207.8	291.7	266.5
8	18	5	59.7	74.4	131	157.7	216.1	257.9	273.1	325.7
9	18	11	59.7	65.4	131	142.3	216.1	230.4	273.1	291.7
10	18	24	59.7	58.4	131	128.9	216.1	207.8	273.1	266.5
11	24	5	58.4	74.4	128.9	157.7	207.8	257.9	266.5	325.7
12	24	11	58.4	65.4	128.9	142.3	207.8	230.4	266.5	291.7
13	24	18	58.4	59.7	128.9	131	207.8	216.1	266.5	273.1

18 % to 24 %. The normalised mode shapes corresponding to the four moisture contents studied have been compared in Fig. 11 for each mode and sensor location. The normalised mode shapes were produced by normalising the peak amplitude to a value of 1. The vertical axis shows the normalised amplitude and the horizontal axis shows the sensor location denoted by DOF. It is seen that moisture content changes have insignificant effects on the mode shapes.

3.5.2. Empirical equation for estimating the arch natural frequencies at different material moisture contents

Natural frequencies are the primary dynamic properties used for structural behaviour studies. A structure may experience different moisture conditions during its operation. In the previous section it was shown that the material moisture content can considerably affect the natural frequencies of the brick masonry semi-circular arch. Since the process of conducting experimental tests for measuring the natural frequencies of a structure at different moisture contents is costly and time-consuming, providing a formula to estimate natural frequencies at different moisture contents is useful in structural studies. To generate such a formula, the obtained experimental data presented in Table 5 for the moisture contents of 5 %, 11 %, 18 %, and 24 % were used. For each two performed tests at two different material moisture contents, the ratio of their natural frequencies ($\frac{f}{f_0}$) and the ratio of material moisture contents ($\frac{m}{m_0}$) were calculated. In this way, 13 sets of data were considered, as presented in Table 6. Table 6 presents the used experimental data, including material moisture contents and arch natural frequencies for fitting the equation. An equation was fitted to these data, as shown in Fig. 12. This process was done for each of the four modes separately. As a

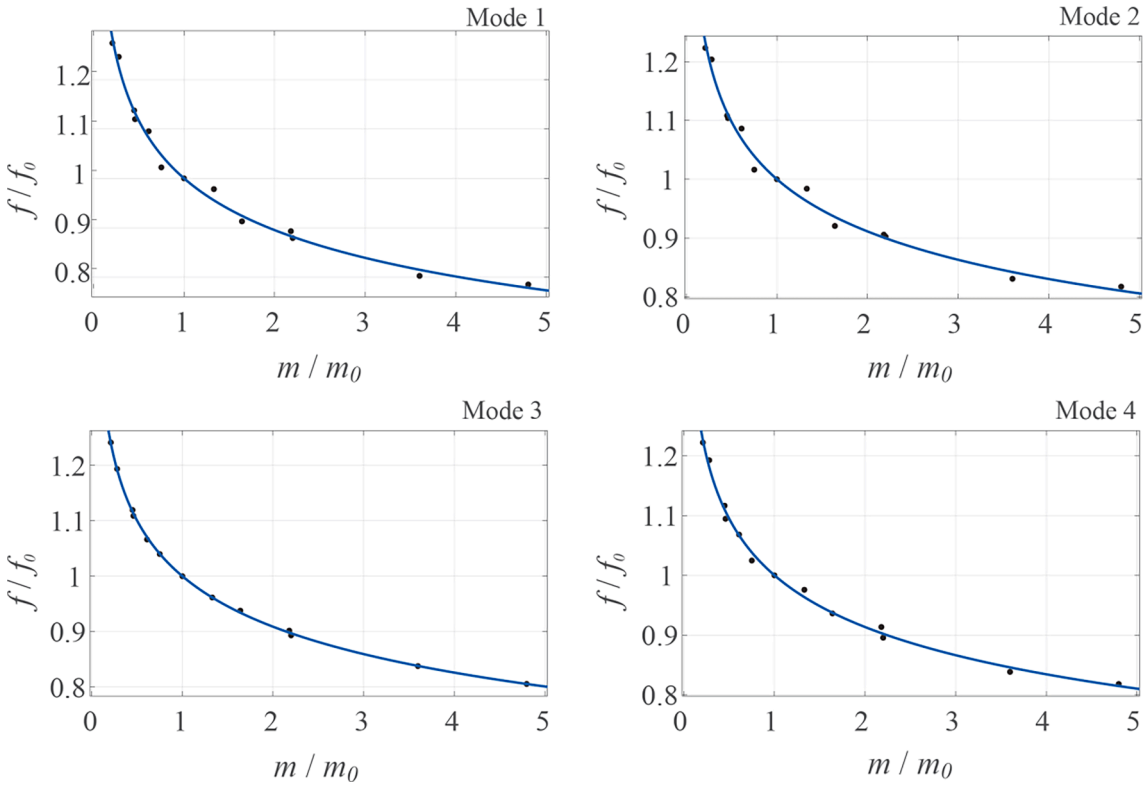

Fig. 12. Fitted equation for each of four modes.

Table 7
The coefficient α_n corresponding to the nth mode.

Mode	1	2	3	4
α_n	0.16	0.13	0.14	0.13

result, the empirical Equation (6) is presented for the semi-circualr arch, which can accurately estimate the natural frequencies at different material moisture contents.

$$f = \left(\frac{m_0}{m}\right)^{\alpha_n} f_0 \tag{6}$$

In Equation (6), n is the mode number, m and m_0 are the moisture contents of material (%) at two conditions, f is the arch natural frequency of the nth mode (Hz) in the situation where the moisture content of material is equal to m, m_0 is the moisture content of material (%) at which the nth natural frequency of the structure (f_0) is measured, and f_0 is the arch natural frequency of the nth mode (Hz) in the situation where the moisture content of material is equal to m_0. The coefficient α_n is the coefficient corresponding to the nth mode, which is given in the Table 7.

The difference between natural frequencies obtained from the experimental tests and estimated frequencies obtained from the empirical Equation (6) for each set of data is depicted in Fig. 13. The number in the first column of Table 7 indicates the corresponding data between Table 6 and Fig. 13. According to these results, the difference is less than 2.5 % in all cases. The coefficient of determination (R^2) of this equation for each of the four modes is more than 0.99, which shows the high accuracy of the proposed equation in estimating the natural frequency at different material moisture contents.

4. Finite element analysis of the semi-circular arch

The mass density and modulus of elasticity of bricks and gypsum mortar (presented in Table 1) were implemented in the FE model of the

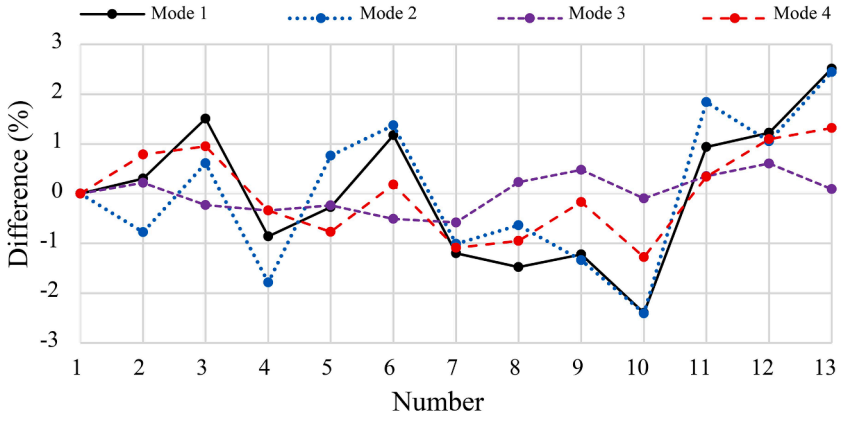

Fig. 13. Difference between experimental data and empirical equation data.

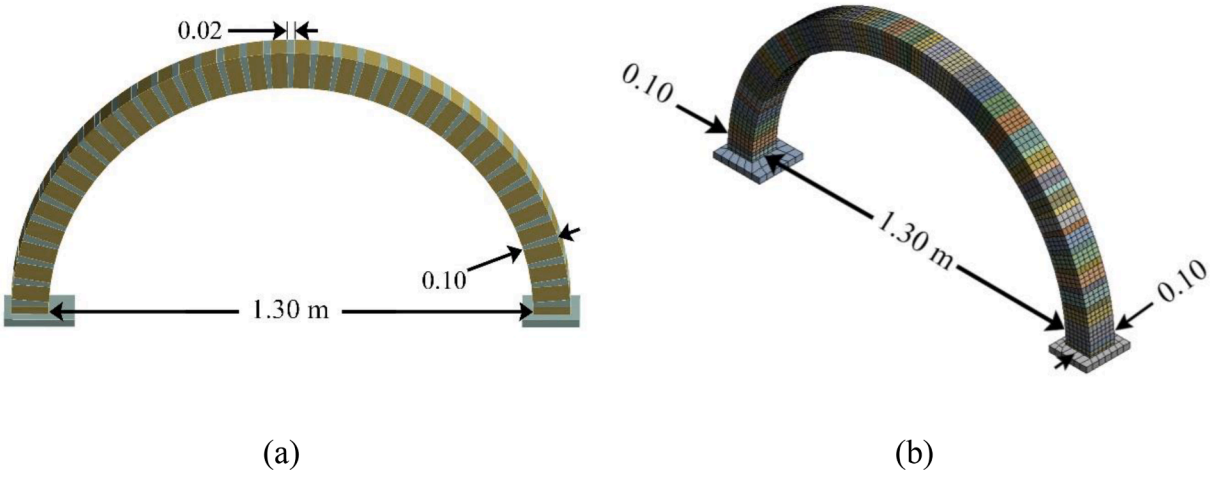

Fig. 14. FE model of the arch: a) overview, b) meshing.

Table 8
Comparison between un-updated finite element and experimental frequencies of the arch.

Mode	Experimental frequencies (Hz)	Un-updated FE frequencies (Hz)	Difference (%)
1	66.4	49.3	35
2	142.5	104.2	37
3	231.3	190.3	22
4	294.1	244.6	20

arch (micro-modelling). The dynamic parameters were obtained during tests on the semi-circular arch. Then, updating and calibrating the FE models made it possible to update some of the materials mechanical properties. In the following, the importance of updating the FE model will be shown and it will be observed that it can make a considerable difference in the FE model response. It should be noted that the objective of FE model updating here is the convergence of the frequencies towards the experimental frequencies by changing the material mechanical properties. To do so, it is not necessary to have the mechanical properties of the materials measured through laboratory tests as the convergence will always occur with any initial value, but having the measured values as the initial values shortens the process of convergence.

For this reason, at normal conditions of the laboratory (temperature of 20 °C and moisture content of 11 %) FE analysis was performed for two cases: 1) the arch with material mechanical properties directly obtained from mechanical tests without updating and 2) the arch with updated material mechanical properties.

The three-dimensional micro-modelling analysis was performed using the FE ANSYS code [36]. The Solid 65 hexahedral element with eight nodes and three translational degrees of freedom at each node was used. The interface between bricks and mortar was modelled by contact and target elements. The linear modal analysis was used.

4.1. The arch finite element model without model updating

Before updating the FE model of the arch, a mesh study was conducted to find the number of elements sufficient for convergence. A precision of 1 % was selected for the convergence of frequencies of the arch using modal analysis, which resulted in 9864 elements (Fig. 14). The first four frequencies and the mode shapes resulted from FE analysis are presented in Table 8 and Fig. 15. The first four FE frequencies range

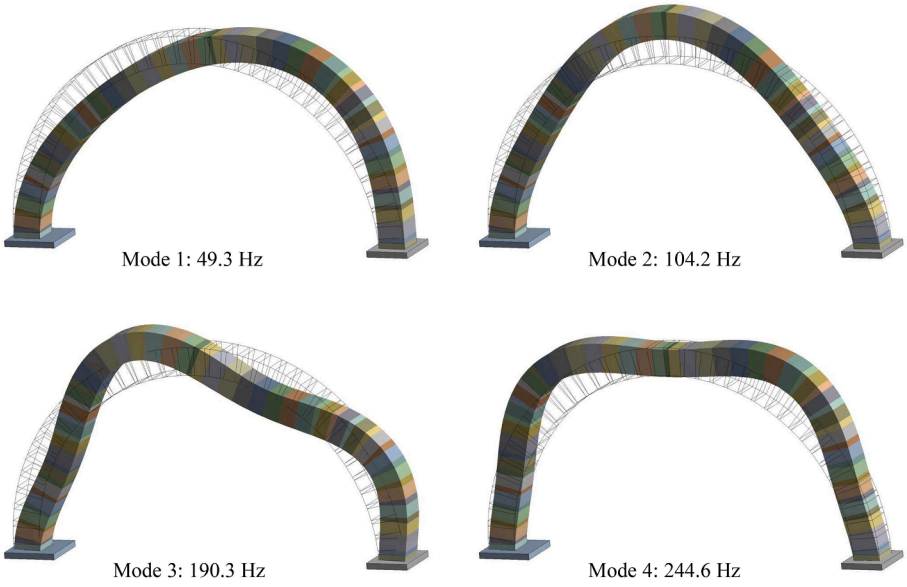

Fig. 15. Un-updated FE natural frequencies and mode shapes of the arch.

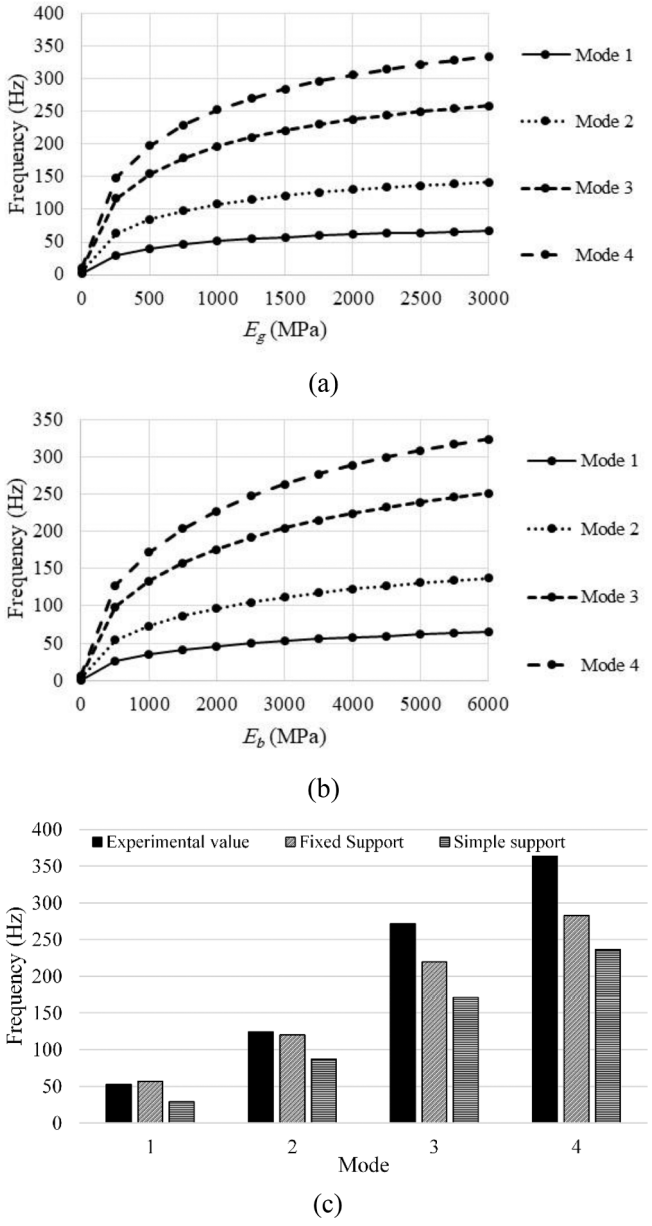

Fig. 16. Variation of the arch natural frequencies versus the variation of updated parameters: a) the modulus of elasticity of the brick, b) the modulus of elasticity of the gypsum mortar, c) type of support.

Table 9
Updated parameters, the initial and final values in FEMU of the arch.

The updated parameters	Initial value	Lower bound	Upper bound	Final value	Difference (%)
E_b (MPa)	4603	5000	5500	5305	+15.25
E_g (MPa)	1658	2000	3000	2180	+31.48
Type of supports	Simple	–	–	Fixed	–

from 49.3 Hz to 294.1 Hz. The comparison between experimental and FE results shows that frequencies from FE analysis are between 20 % and 37 % less than the experimental ones. Therefore, the FE model needs to be updated to result in dynamics response close to the experiment.

4.2. The arch finite element model updating

The FEMU reduces the difference between the numerical and experimental dynamic parameters, such as frequencies and mode shapes. Parameters considered for updating the FE model of the semi-circular arch include the modulus of elasticity and Poisson's ratio of the brick, the gypsum mortar, and the supports fixity of the arch. The arch was placed on a concrete floor in the laboratory. Supports were connected to the floor with gypsum mortar (Fig. 4(a)). Two cases were considered in the FE model to investigate the effect of the fixity of the supports of the arch. In the first case, fixed supports were defined by confining the three displacements of all nodes of the supports. In the second case, the three displacements of only the centre-lines of the supports perpendicular to the arch plane were confined to simulate the condition of simple supports.

To have an initial estimation of the effect of each parameter, one of the parameters was considered as a variable each time. Meanwhile, other parameters were assumed to be temporarily constant and equal to the initial values obtained from the experimental tests, presented in Section 3. The modulus of elasticity and Poisson's ratios increased from zero until the resulting frequencies reached the dynamic test values. Fig. 16(a) and (b) show the frequency changes and its significant sensitivity during the changes in the modulus of elasticity of the brick and the gypsum mortar, respectively. The modulus of elasticity increased from 1 MPa to 6000 MPa for the brick and from 1 MPa to 3000 MPa for the gypsum mortar. The results show that increasing just one of the modules of elasticity of brick or mortar cannot increase the frequencies more than a specific value. In other words, the slope of the frequency versus modulus of elasticity diagram gradually decreases by increasing the modulus of elasticity.

The objective function (Equation (1)) presented in Section 2 was used during the trial-and-error process to bring the updated FE results closer to experimental results. The Trust-Region Gauss-Newton method was used for optimisation. Fig. 16(a) and (b) indicate that the range of 2000 MPa to 3000 MPa for the mortar modulus of elasticity (E_g), and 5000 MPa to 5500 MPa for brick modulus of elasticity (E_b) are the ranges that the rate of change of each modulus of elasticity has dramatically increased and it approaches to the convergence.

The effect of changing the Poisson's ratio on dynamic parameters of the arch is negligible. Changing the Poisson's ratio from 0.01 to 0.49 affects the natural frequencies, less than 0.8 %.

Fig. 16(c) shows that the assumption of the fixed support considered for both supports of the arch in the FE model gives natural frequencies closer to experimental results (with the average difference of −13.4 %) than the assumption of simple supports (with the average difference of −35.3 %).

The initial, lower and upper bounds and final values of updated parameters for the arch during FEMU are presented in Table 9. The final modulus of elasticity of brick and gypsum mortar are respectively suggested as 5305 MPa and 2180 MPa. Fixed supports create more accurate results. The final values can be used for more accurate FE modelling and further analysis of these structures. There is no specific suggestion for Poisson's ratio in Table 9 due to its negligible effect on the studied arch dynamic parameters.

The natural frequencies of updated FE models of the arch are presented in Table 10. The differences between un-updated and updated frequencies with the experimental values are also given. The main reason for these differences in frequencies of the two updated and un-updated models is related to the difference in the type of supports and the difference in modulus of elasticity of brick and gypsum mortar in modelling. The average of the frequency differences between updated models and experimental values after FEMU are −0.3 %, while they are −21.8 % for un-updated models. Fig. 17 shows that there is a good agreement between FE frequencies and experimental frequencies after updating.

4.3. Future research work

This paper studied the effect of changes in temperature and moisture

Table 10
Comparison between experimental, un-updated and updated FE model frequencies of the arch.

Mode	Un-updated model frequencies (Hz)	Updated model frequencies (Hz)	Experimental frequencies (Hz)	Frequency difference of un-updated model and experiment (%)	Frequency difference of updated model and experiment (%)
1	49.3	62.8	66.4	−25.8	−5.4
2	104.2	132.9	142.5	−26.9	−6.7
3	190.3	242.5	231.3	−17.7	4.8
4	244.6	312.6	294.1	−16.8	6.3
			Average	−21.8	−0.3

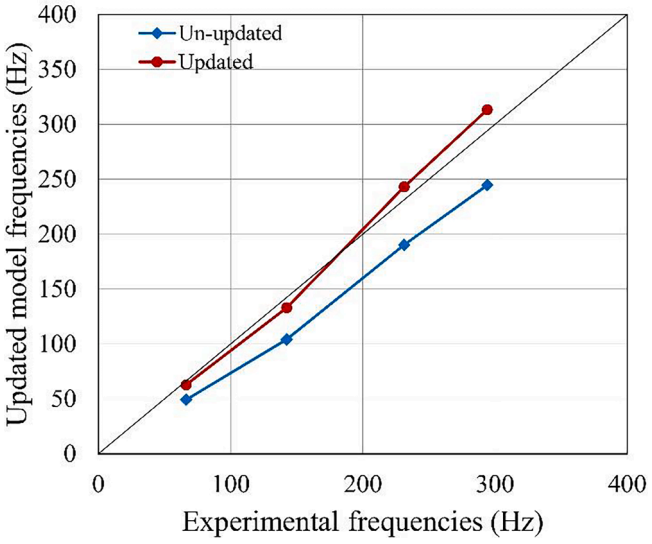

Fig. 17. Comparative frequencies diagram of un-updated and updated arches versus experimental values.

content on the dynamic properties of semi-circular brick masonry arches. The obtained results can be developed by performing further studies, which may include investigating other affecting parameters such as the temperature and moisture during arch construction process, material and arch curing conditions, the ratio of mortar thickness to brick thickness, arches with a variable thickness, and arches with other types of construction materials. The presence of damage in the arch is another aspect of research.

It is also recommended to survey other types of traditional arches of different geometrical dimensions in order to develop equations to estimate the natural frequencies of these arches based on their geometric characteristics. Integrating the equations developed in future with the equations related to the natural frequency estimation presented in this study can reduce the need for laboratory tests of the arches in different conditions. It should also be noted that the provided equation in this study for different material moisture contents is limited to the semi-circular arch and the obtained results in this study. Therefore, there is a need for more examination of this equation for different arch types in different conditions.

Results for the relationship between the static and dynamic moduli of elasticity obtained from FEMU in this study is limited to the materials, clay brick and gypsum mortar, used in the arch studied. Other types of materials with different ranges of mechanical properties should be tested and then numerically simulated to obtain holistic results.

The geometrical shape of the arch studied is semi-circular. Arches with other geometrical shapes should be tested and simulated for understanding the effect of the geometry of the arch on its dynamic parameters.

5. Conclusions

In this paper, the effect of changes in temperature and moisture content on the dynamic behaviour of semi-circular brick masonry arches was studied. A brick masonry arch with gypsum mortar was built in the laboratory for this purpose. Mechanical properties of constituent materials, including brick, gypsum mortar, and their assemblage, were measured first in the laboratory. The compressive strength, modulus of elasticity, and stress–strain relationships were obtained for them. Then, the dynamic parameters of the arch, including natural frequencies, modal damping ratios and mode shapes, were calculated by dynamic identification through the OMA after changing each intended condition.

The study showed that the dynamic properties of semi-circular clay brick masonry arches is very sensitive to the test conditions. The effect of conditions must be considered on the obtained results from the dynamic identification process.

The temperature changes had somewhat unpredictable effects on dynamic parameters in different modes. However, the difference is in specific ranges, as reported.

The moisture content had regular effects on dynamic behaviour. For this reason, its effect can be predicted by measuring it during dynamic tests. An increase in the moisture content caused a reduction in the natural frequencies, but moisture content changes did not considerably affect the mode shapes. The ratios of material moisture contents and the ratios of their corresponding arch natural frequencies obtained from the experiment were considered. Thereafter, an empirical equation was fitted to these ratios to be used for estimating the natural frequencies of the semi-circular arch at different material moisture contents. The comparison of the results of the proposed empirical equation with the results from the test approved the satisfactory accuracy of the equation for the examined arch.

The FEMU was used to calibrate the FE model and find the appropriate values for the brick and mortar modulus of elasticity in the dynamic condition. It was shown that using the modulus of elasticity from static (non-dynamic) tests can cause more than a 10 % difference in the natural frequency of the FE model. This is a significant difference that can make numerical modelling unreliable. To prevent this, first, it is better to do FEMU before the use of each FE model for dynamic uses. If this is not possible, it is better to correct the modulus of elasticity values with correction coefficients. For the materials and the arch used in this research, the static modulus of elasticity of clay brick and gypsum mortar must be multiplied by 1.15 and 1.31, respectively, to be used in the FE model for dynamic analysis.

It was concluded that the Poisson's ratio has negligible effects on the dynamic parameters of the arch.

The results showed that when there is an adequate connection between the arch and its supports, the assumption of fixed support is acceptable in FE analysis in the absence of accurate information about the supports conditions.

Obtained results for the effect of temperature in this study are valid only for the range of temperature from 14 °C or 38 °C, due to laboratory equipment limitations for changing the temperature. In real cases, the temperature may range between about −10 °C in the winter and more than 50 °C in the summer, for which additional investigation is needed.

6. Code Availability Statement

Not applicable.

Funding

Not applicable.

Declaration of Competing Interest

The authors declare that they have no known competing financial interests or personal relationships that could have appeared to influence the work reported in this paper.

References

[1] He J, Fu Z. Modal Analysis. Amsterdam: Elsevier; 2001. doi: 10.1016/b978-075065079-3/50001-2.
[2] Jaishi B, Ren W, Zong Z, Maskey PN. Dynamic and seismic performance of old multi-tiered temples in Nepal. Eng Struct 2003;25:1827–39. https://doi.org/10.1016/J.ENGSTRUCT.2003.08.006.
[3] De Sortis A, Antonacci E, Vestroni F. Dynamic identification of a masonry building using forced vibration tests. Eng Struct 2005;27:155–65. https://doi.org/10.1016/J.ENGSTRUCT.2004.08.012.
[4] Ramos LF, Marques L, Lourenço PB, De Roeck G, Campos-Costa A, Roque J. Monitoring historical masonry structures with operational modal analysis: two case studies. Mech Syst Sig Process 2010;24:1291–305. https://doi.org/10.1016/J.YMSSP.2010.01.011.
[5] Gentile C, Saisi A. Ambient vibration testing of historic masonry towers for structural identification and damage assessment. Constr Build Mater 2007;21:1311–21. https://doi.org/10.1016/j.conbuildmat.2006.01.007.
[6] Rebelo C, Júlio E, Costa D. Modal identification of the coimbra university tower. Proc. 2nd Int. Oper. Modal Anal. Conf., Copenhagen: 2007, p. 177–84.
[7] Ivorra S, Pallarés F. A masonry bell-tower assessment by modal testing. Proc. 2nd Int. Oper. Modal Anal. Conf., vol. 30, Copenhagen: 2007.
[8] Makarios T. Identification of building dynamic characteristics by using the modal response acceleration time-histories in the seismic excitation and the wind dynamic loading cases. CHAPTER 4 of Book "Accelerometers; Principles,Structure and Applications". 1st ed., New York: Nova Science Publisher; 2013, p. 77–114.
[9] Makarios T. Identification of the mode shapes of spatial tall multi-storey buildings due to earthquakes: the new 'modal time-histories' method. Struct Design Tall Spec Build 2012;21:621–41. https://doi.org/10.1002/TAL.630.
[10] Foti D, Diaferio M, Giannoccaro NI, Mongelli M. Ambient vibration testing, dynamic identification and model updating of a historic tower. NDT and E Int 2012;47:88–95. https://doi.org/10.1016/j.ndteint.2011.11.009.
[11] Gentile C, Saisi A. Operational modal testing of historic structures at different levels of excitation. Constr Build Mater 2013;48:1273–85. https://doi.org/10.1016/j.conbuildmat.2013.01.013.
[12] Masciotta MG, Ramos LF, Lourenço PB, Vasta M. Structural monitoring and damage identification on a masonry chimney by a spectral-based identification technique. Proc EURODYN 2014–9th Int Conf Struct Dyn, Porto 2014:211–8.
[13] Valvona F, Toti J, Gattulli V, Potenza F. Effective seismic strengthening and monitoring of a masonry vault by using Glass Fiber Reinforced Cementitious Matrix with embedded Fiber Bragg Grating sensors. Compos B Eng 2017;113:355–70. https://doi.org/10.1016/J.COMPOSITESB.2017.01.024.
[14] Mesquita E, Arêde A, Silva R, Rocha P, Gomes A, Pinto N, et al. Structural health monitoring of the retrofitting process, characterization and reliability analysis of a masonry heritage construction. J Civ Struct Heal Monit 2017;7(3):405–28.
[15] Cavalagli N, Comanducci G, Ubertini F. Earthquake-induced damage detection in a monumental masonry bell-tower using long-term dynamic monitoring data. J Earthq Eng 2018;22:96–119. https://doi.org/10.1080/13632469.2017.1323048.
[16] Vincenzi L, Bassoli E, Ponsi F, Castagnetti C, Mancini F. Dynamic monitoring and evaluation of bell ringing effects for the structural assessment of a masonry bell tower. J Civ Struct Heal Monit 2019;9:439–58. https://doi.org/10.1007/s13349-019-00344-9.
[17] Bianchini N, Mendes N, Lourenço P. Seismic evaluation of Bagan heritage site (Myanmar): The Loka-Hteik-Pan temple. Structures 2020;24:905–21. https://doi.org/10.1016/J.ISTRUC.2020.01.020.
[18] Onat O. Impact of mechanical properties of historical masonry bridges on fundamental vibration frequency. Structures 2020;27:1011–28. https://doi.org/10.1016/j.istruc.2020.07.014.
[19] Nochebuena-Mora E, Mendes N, Lourenço PB, Greco F. Dynamic behavior of a masonry bell tower subjected to actions caused by bell swinging. Structures 2021;34:1798–810. https://doi.org/10.1016/J.ISTRUC.2021.08.066.
[20] Calayır Y, Yetkin M, Erkek H. Finite element model updating of masonry minarets by using operational modal analysis method. Structures 2021;34:3501–7. https://doi.org/10.1016/J.ISTRUC.2021.09.103.
[21] Gonen S, Soyoz S. Investigations on the elasticity modulus of stone masonry. Structures 2021;30:378–89. https://doi.org/10.1016/J.ISTRUC.2021.01.035.
[22] Ni P, Li Q, Han Q, Xu K, Du X. Substructure approach for Bayesian probabilistic model updating using response reconstruction technique. Mech Syst Sig Process 2023;183:109632. https://doi.org/10.1016/J.YMSSP.2022.109624.
[23] Han Q, Ni P, Du X, Zhou H, Cheng X. Computationally efficient Bayesian inference for probabilistic model updating with polynomial chaos and Gibbs sampling. Struct Control Health Monit 2022;29:e2944.
[24] Ni P, Han Q, Du X, Cheng X. Bayesian model updating of civil structures with likelihood-free inference approach and response reconstruction technique. Mech Syst Sig Process 2022;164:108212. https://doi.org/10.1016/J.YMSSP.2021.108204.
[25] Peeters B. System identification and damage detection in civil engineering. Katholieke Universiteit Leuven; 2000.
[26] Brincker R, Andersen P, Cantieni R. Identification and level I damage detection of the Z24 highway bridge. Exp Tech 2001;25:51–7. https://doi.org/10.1111/j.1747-1567.2001.tb00047.x.
[27] Lynch JP, Law KH, Kiremidjian A, Kenny T, Carryer E. A wireless modular monitoring system for civil structures. In: Yasinn, editor. Proc. 20th Int. Modal Anal. Conf. Struct. Dyn., vol. 4753, Los Angeles, CA: 2002, p. 1–6.
[28] Teughels A. Inverse modelling of civil engineering structures based on operational modal data. Belgium: Catholic University of Leuven; 2004. Ph.D. thesis.
[29] Methods of Test for Masonry Units - Part 1: Determination of Compressive Strength. BSI BS EN 772-1; 2000.
[30] BSI, BS EN 13279-2: Gypsum binders and gypsum plasters Part 2: Test methods. British Standards Institution 2014.
[31] Methods of Test for Masonry – Determination of Compressive Strength. BSI BS EN 1052-1; 1999.
[32] Plachy T, Tesarek P, Padevet P, Polak M. Determination of Young's modulus of gypsum blocks using two different experimental methods. Mathematics and Computers in Science and Engineering 2009;32:456–68.
[33] Ramos LF, De Roeck G, Lourenço PB, Campos-Costa A. Damage identification on arched masonry structures using ambient and random impact vibrations. Eng Struct 2010;32:146–62. https://doi.org/10.1016/j.engstruct.2009.09.002.
[34] Deraemaeker A, Reynders E, De Roeck G, Kullaa J. Vibration-based structural health monitoring using output-only measurements under changing environment. Mech Syst Sig Process 2008;22:34–56. https://doi.org/10.1016/j.ymssp.2007.07.004.
[35] Farrar CR, Worden K. An introduction to structural health monitoring. Philos Trans R Soc A Math Phys Eng Sci 2007;365:303–15. https://doi.org/10.1098/rsta.2006.1928.
[36] Basic Analysis Guide for ANSYS 20. New York: SAS IP Inc.; 2020.